



MISSOURI  
**S&T**

# CENTER FOR TRANSPORTATION INFRASTRUCTURE AND SAFETY

## **Seismic Retrofit of CISS Column Foundation Shafts to Bent Cap Connections**

by

Pedro F. Silva, Michael Lubiewski, and Genda Chen



**NUTC  
R203**

**A National University Transportation Center  
at Missouri University of Science & Technology**

## ***Disclaimer***

The contents of this report reflect the views of the author(s), who are responsible for the facts and the accuracy of information presented herein. This document is disseminated under the sponsorship of the Department of Transportation, University Transportation Centers Program and the Center for Infrastructure Engineering Studies UTC program at the University of Missouri - Rolla, in the interest of information exchange. The U.S. Government and Center for Infrastructure Engineering Studies assumes no liability for the contents or use thereof.

### Technical Report Documentation Page

1. Report No.  NUTC R203	2. Government Accession No.	3. Recipient's Catalog No.	
4. Title and Subtitle  Seismic Retrofit of CISS Column Foundation Shafts to Bent Cap Connections		5. Report Date  April 2008	
		6. Performing Organization Code	
7. Author/s  Pedro F. Silva, Michael Lubiewski, and Genda Chen		8. Performing Organization Report No.  00016751	
9. Performing Organization Name and Address  Center for Transportation Infrastructure and Safety/NUTC program Missouri University of Science & Technology 223 Engineering Research Lab Rolla, MO 65409		10. Work Unit No. (TRAIS)	
		11. Contract or Grant No.  DTRT06-G-0014	
12. Sponsoring Organization Name and Address  U.S. Department of Transportation Research and Special Programs Administration 400 7 <sup>th</sup> Street, SW Washington, DC 20590-0001		13. Type of Report and Period Covered  Final	
		14. Sponsoring Agency Code	
15. Supplementary Notes			
16. Abstract  An upgrade method for improving the seismic performance of typical bridges built in the state of Alaska is presented herein. This work studied the feasibility of the upgrade method for direct implementation in the field. Three specimens consisting of a cast in place steel shell (CISS) column foundation shaft and a bent cap configured to form a tee connection were built to model a typical bridge bent and tested under simulated seismic loads. Each specimen was retrofitted in the column, bent cap, and their connection according to current seismic design standards. This paper presents key experimental results, and the philosophy used in the design of the test units.			
17. Key Words  Seismic design, joint shear design, CISS shafts, capacity design	18. Distribution Statement  No restrictions. This document is available to the public through the National Technical Information Service, Springfield, Virginia 22161.		
19. Security Classification (of this report)  unclassified	20. Security Classification (of this page)  unclassified	21. No. Of Pages  36	22. Price

# **Seismic Retrofit of CISS Column Foundation Shafts to Bent Cap Connections**

by

Pedro F. Silva, Michael Lubiewski, and Genda Chen

**Biography:** ACI member **P. F. Silva** is an Associate Professor of Civil and Environmental Engineering at the George Washington University, DC. He is a member of the ACI Committees 440, and 341. His research interests include the development of innovative performance-based procedures for the design and retrofit of structures, and use of fiber reinforcement polymers for the structural rehabilitation of structures.

**M. C. Lubiewski** is a structural Engineer with Walter P. Moore in Kansas City, MO. His research interests include the structural rehabilitation and nonlinear analysis of structures.

**G. D. Chen** is a Professor at the University of Missouri-Rolla. He is a member of ASCE and EERI. His research interests include the seismic design and retrofit of buildings and bridges with steel and composite materials, damage detection of RC members and structures, and dynamic response modification of structures with innovative devices and systems.

## **ABSTRACT**

An upgrade method for improving the seismic performance of typical bridges built in the state of Alaska is presented herein. This work studied the feasibility of the upgrade method for direct implementation in the field. Three specimens consisting of a cast in place steel shell (CISS) column foundation shaft and a bent cap configured to form a tee connection were built to model a typical bridge bent and tested under simulated seismic loads. Each specimen was retrofitted in the column, bent cap, and their connection according to current seismic design standards. This paper presents key experimental results, and the philosophy used in the design of the test units.

**Keywords:** seismic design, joint shear design, CISS shafts, capacity design

## INTRODUCTION

Previous research has shown that existing bridges built in the state of Alaska may be prone to undesirable failure modes when subjected to seismic loads. Based on an evaluation of bridges built in the state of Alaska (Silva *et al.*, 1999), identified design deficiencies common to these as-built bridges are: *i)* the CISS column foundation shafts have excessive longitudinal reinforcement ratios, *ii)* the bent cap yield moment capacity is below the maximum feasible moment that develops at the column faces, *iii)* the steel shells are partially embedded in the joint region, and *iv)* the bent cap have inadequate amounts of joint shear reinforcement to sustain the levels of principal tensile stresses that develop in the joint.

Under seismic loading, these design deficiencies lead to a poor seismic response, does not meet current capacity design standards (AASHTO, 1998; Caltrans, 2004; Priestley *et al.*, 1995), and there is a need to develop procedures for the seismic upgrade of these systems. In the last decades researchers have developed a number of retrofit options for joints that were considered in this research program.

These may include external prestressing of the bent cap and joint in the longitudinal direction. This retrofit strategy was investigated extensively by Ingham *et al.* (1994), resulting in an improved joint response. In this work prestressing was also evaluated; but the bent cap was only prestressed in the transverse direction. Unlike longitudinal prestressing, transverse prestressing only merits by increasing the strength capacity of the joint to resist the input tensile stresses, but it does not lead either to a reduction in the principle tensile stresses nor does it increases the shear and flexural strength of the bent cap. Although not as effective as prestressing in the longitudinal direction, it is a reasonable alternative and since it has not been previously investigated, merits investigation for its usefulness in field applications.

Other retrofit strategies involved encasing the as-built joints in concrete (Ingham *et al.*; 1994), steel (Alcocer and Jirsa, 1993) or more recently, FRP composites jacketing (Pantelides *et al.*, 2004; Silva *et al.*, 2007). In their report Ingham *et al.* (1994), have also investigated the process of complete joint replacement. Other alternatives implemented the process of constructing link beams as a means for seismic upgrade (Priestley *et al.*, 1993). In this research program a prototype specimen consisting of an interior column and corresponding bent cap was designed and constructed in a T-configuration by including the aforementioned deficiencies in order to investigate seismic improvements and propose procedures for field implementation. Briefly, the details investigated included:

*i)* The moment capacity of the column was reduced by cutting a portion of the column longitudinal reinforcement at the connection to the bent cap to levels that can ensure a proper ductile seismic response;

*ii)* A section of the steel shell was cut and removed leaving a gap between the steel shell and the bent cap. The steel shell was removed to provide access to cut the column longitudinal reinforcement thereby reducing the reinforcement ratio as designated above. Previous research has also shown that leaving this gap avoids significant damage to the bent cap under small rotations because the prying action of the steel shell against the surrounding concrete is avoided (Silva *et al.*, 1999);

*iii)* The bent cap dimensions were increased with a concrete jacket to ensure proper reinforcement spacing and to install the additional flexure and joint shear reinforcement (Sritharan, 2005). Increasing the bent cap also leads to a reduction in the principle tensile stresses and provides a better transfer of stresses within the joint region. Enlarging the bent cap also provides a greater development length of the column longitudinal reinforcement, thereby

increasing the anchorage capacity of this reinforcement. Lastly, the bent cap was enlarged to levels that can prevent reinforcement congestion within the joint region, and in one of the test units transverse prestressing was also investigated.

Construction and design implementation of these details are discussed in greater detail in the paper. Results from a cyclic testing of the upgraded specimens showed a ductile response up to the displacement ductility 4 for the three specimens without significant decreases in the strength of the test units. Beyond this ductility, the main failure mode of Unit 1 was attributed to joint shear failure due to excessive transverse dilations in the joint region. An improved joint detail was implemented for Unit 2, and the main failure mode was attributed to low cyclic fatigue of the column longitudinal reinforcement. However, extensive joint degradation was recorded beyond ductility 6. In Unit 3 the joint was post-tensioned in the transverse direction while also decreasing the gap length between the steel shell and the bent cap. Beyond ductility 6 degradation of the lateral load capacity of the column occurred due to joint shear failure. Detailed design description of these units and experimental results are discussed herein.

## **RESEARCH SIGNIFICANCE**

This research investigated deficiencies of typical bridges built in the state of Alaska when placed under seismic loads. An upgrade method for improving the seismic performance of these bridges was proposed and experimentally investigated. A laboratory model was designed, constructed, and tested under simulated seismic loads with the main goal of investigating the feasibility for field implementation of the proposed upgrade scheme.

## **TEST SETUP**

Three specimens consisting of a cast in place steel shell (CISS) column foundation shaft and a bent cap configured to form a tee connection were built and tested according to the setup shown

in Figure 1. Construction of the units was performed in two phases. Construction of the as-built section was accomplished in the first phase, while in the second phase, the as-built portion was modified as needed and the new retrofit section was added. The as-built sections were constructed in a similar manner as in field conditions; however, in order to ensure proper safety precautions each unit was built in an inverted position, as shown in Figure 1(b). The effective column height was 2.72 m (8.9ft) and the total axial load was 710kN (169kips) or an axial load ratio of 8%. Further test setup details maybe found in Figure 1 and (Silva *et al.*, 2007).

## **MATERIAL PROPERTIES**

Analytical investigations are presented in detail in the next few sections. A detailed list of all the material properties used in these analyses is presented in Table 1 to Table 3. Concrete cylinders were cast for each lift of concrete and stored next to the test unit. Rebar samples were taken from each lot of steel and tested. All material tests for either the concrete or reinforcing steel were obtained from sets of three and are reported in these tables as the average values.

## **AS-BUILT SPECIMEN REINFORCEMENT LAYOUT AND FABRICATION**

### **COLUMN REINFORCEMENT**

As shown in Figure 2(a), the as-built longitudinal reinforcement consisted of 20–D32 (#10) bars that were encased in a 13mm (1/2in.) thick steel shell with a concrete cover of 51mm (2in.) leading to a reinforcement ratio of 6.1%. Furthermore, the steel shell was embedded 89mm (2.25in.) into the bent cap and the anchorage length of the longitudinal reinforcement was 690mm (27.2in.). The transverse reinforcement was provided only for construction purposes and consisted of D10 (#3) hoops at 381mm (15in.) on center.

### **BENT CAP REINFORCEMENT**

The top and bottom main longitudinal reinforcement consisted of 8-D16 (#5) placed in two rows.



The transverse reinforcement consisted of closed D13 (#4) stirrups spaced at 254mm (10in.), see Figure 2(a). Matching the as-built bent cap, no transverse reinforcement was provided within the joint region. This detail does not comply with current seismic design standards (AASHTO, 1998; Caltrans, 2004), and this issue was addressed in this research.

### **SEISMIC DESIGN CONSIDERATIONS FOR THE RETROFIT/UPGRADE SECTION**

After the as-built section was constructed, modifications were implemented according to well established seismic design principles to improve the unit's seismic performance.

#### **COLUMN DESIGN CONSIDERATIONS**

The longitudinal reinforcement was reduced to a reinforcement ratio below 4.0%. This reinforcement ratio was suggested in order to avoid excessive amounts of joint shear reinforcement that can lead to reinforcement congestion within the joint region (Priestley *et al.*, 1995). In order to access the longitudinal reinforcement, the steel shell was cut leaving a gap between the steel shell and the new bent cap section interface, as shown in Figure 2(b) and (c). In Figure 2(b) and Figure 3(a) the gap was 51mm (2in.) for Units 1 and 2, and in Figure 3(c) the gap was reduced to 13mm (0.50in.) for Unit 3. The main considerations for reducing this gap region are explained later while discussing the experimental results.

After cutting the steel shell the reinforcement was exposed, and 8 column bars in total bars were cut immediately above the as-built bent cap section. The new column section consisted of 12-D32 (#10) longitudinal reinforcement, thereby reducing the reinforcement ratio from 6.1 % to 3.7%. This new column reinforcement ratio was identical for all three test units, and was used to design the flexural, shear, and joint shear reinforcement for the new bent cap according to well established capacity design principles.

## Column Moment-Curvature Analysis

A moment-curvature analysis was performed for the as-built and the retrofitted column sections. For the as-built section, the internal forces within the compression zone consisted of forces in the concrete, the longitudinal reinforcement and the steel shell. Within the tension block, only the longitudinal reinforcement was considered effective in transferring forces. An expression has been previously evaluated in a research program by Silva and Seible (2001) and is:

$$\sum_{i=1}^{nc} \alpha_i f_{ci} A_{ci} + \sum_{i=1}^{ns} f_{si} A_{si} + \sum_{i=1}^{nc} \alpha_i f_{shi} A_{shi} = P \quad (1)$$

In Eq. (1) the concrete stresses,  $f_{ci}$ , were also evaluated considering the confining action of the steel shell (Silva and Seible, 2001).

For the retrofitted section and because of the steel shell gap above the bent cap interface, the moment-curvature analysis was implemented considering that in the compression block only the concrete and longitudinal reinforcement are effective in transferring forces and is given by (Silva and Seible, 2001)

$$\sum_{i=1}^{nc} \alpha_i f_{ci} A_{ci} + \sum_{i=1}^{ns} f_{si} A_{si} = P \quad (2)$$

For Units 1 and 2, the concrete compression block was assumed confined by an equivalent spiral section with a size and pitch of 13x13mm (0.50x0.50in.) and 51mm (2in.), respectively. These numbers correspond to the steel shell thickness and the gap at the interface with the bent cap, as shown in Figure 2(b) and Figure 3(a). For Unit 3 and because of the reduced gap, the equivalent spiral size and pitch were 13x13mm (0.50x0.50in.) and 13mm (0.50in.), respectively.

Figure 4(a) shows the retrofitted sections moment capacity (i.e. 3.7%) for Units 1 and 2, and Unit 3. The slight increase in Unit 3 moment capacity results from the decrease in the gap size and the equivalent spiral pitch.

## **BENT CAP DESIGN CONSIDERATIONS**

The maximum moment demand imposed on the bent cap was determined based on the ultimate moment capacity of the reduced column reinforcement ratio of 3.7%, the applied axial load, and the structural model presented in Figure 4 (c). The moment demand imposed on the bent cap was computed at nodes *E* and *F*, corresponding to the column interface. Since in the test units the negative bending moment capacity was higher than the positive bending moment demand (at the interface of the column), only the results for the positive bending moment are presented.

### **Bent Cap Moment-Curvature Analysis**

The bent cap demand analysis is presented in Figure 4(d) and the numerical values described in Table 4. Results from this analysis show that the  $M'_y=464\text{kN}\cdot\text{m}$  (343kips-ft), is considerably lower than Unit 3 maximum probable moment demand of 1,051kN-m (775kips-ft). These results indicate that significant inelastic deformations were likely to develop in the as-built bent cap. As such, additional reinforcement was added to the beam to increase its yield capacity.

Additional longitudinal reinforcement in the amount of approximately  $800\text{mm}^2$  ( $1.24\text{in.}^2$ ) top and bottom were required along with increasing the bent cap dimensions. This limit required a total of 3-D19 (#6) bars. This new bent cap longitudinal reinforcement was identical for all three test units. As shown in Figure 2(b) and Figure 3, the total amount of additional reinforcement provided in the bent cap was 10-D19 (#6) on the top and 12-D19 (#6) on the bottom. These values exceed the required limit because of joint shear design considerations.

Using the new bent cap dimensions along with the existing reinforcement layout shown in Figure 2(b) but only the required 3-D19 (#6) bars placed on top and bottom, the new bent cap section first yield moment was 1,190kN-m (878kips-ft). This suggests that only minor flexural cracks with no yielding of the flexural reinforcement was expected for the new bent cap.

## Bent Cap Sizing

In order to install the required levels of longitudinal reinforcement in the bent cap and to meet current seismic design standards, the required minimum width of the bent cap,  $W_b$ , was

$$W_b = 1.5D_c = 876 \text{ mm (34.5in.)} \quad (3)$$

In order to meet current ACI (2005) bar spacing and cover concrete specifications the required width of the bent cap was increased to 1,055mm (41.5in.). The height of the bent cap was determined based on limits to provide adequate anchorage length for the column longitudinal reinforcement. Using Priestley's *et al.* (1995) recommendations, the development length,  $l_d$ , was computed based on the expression

$$l_d = 0.3d_b \frac{f_{y,c}}{\sqrt{f'_{c,b}}} \approx 677 \text{ mm (26.7in.)} \quad (4)$$

Since the as-built bent cap section provided only for a development length of 629mm (24.8in.), the height of the bent cap was also increased to meet this limit. The new bent cap height was increased to 895mm (35.3in.) and was identical for all three test units.

## JOINT DESIGN CONSIDERATIONS

### Joint Principle Stress Evaluation

Priestley *et al.* (1995) recommends these limits to establish a criterion for the design of joints.

$$p_c \leq 0.3f'_c \quad (5)$$

$$p_t \leq 0.29\sqrt{f'_c} \text{ (MPa)} \quad \left[ 3.5\sqrt{f'_c} \text{ (psi)} \right] \quad (6)$$

$$p_t \geq 0.42\sqrt{f'_c} \text{ (MPa)} \quad \left[ 5.0\sqrt{f'_c} \text{ (psi)} \right] \quad (7)$$

The principle compressive stress limit,  $p_c$ , stipulated by Eq. (5), corresponds to the value at which crushing of the diagonal compression strut through the joint region initiates. The joints were redesigned to ensure that the computed principle compressive stresses were below this

value. The principle tensile stress limit,  $p_t$ , stipulated by Eq. (6) indicates the limit at which diagonal cracking in the joint is initiated and nominal joint shear reinforcement is required. Finally, Eq. (7) stipulates the principle tensile stress limit,  $p_t$ , at which full joint shear reinforcement is required. Interpolation between nominal and full joint shear reinforcement is typically required between these two limits.

Given the applied axial load in the column of 710kN (160kips), the retrofitted column's predicted ultimate moment capacity of 1,588kN-m (1,171kips-ft), see Figure 4(a), and the bent cap height and width of 895mm (35.3in.) and 1,055mm (41.5in.), see Figure 1(a), the joint shearing stress,  $v_j$ , and the axial stress,  $f_a$ , are respectively

$$v_j = \frac{M_u / (0.8H_b)}{\sqrt{2}D_c^2} = 4.09 \text{ MPa (590 psi)} \text{ and} \quad (8)$$

$$f_a = \frac{P}{\sqrt{2}D_c W_b} = 0.82 \text{ MPa (120 psi)}$$

From a Mohr's circle of analysis the maximum principle stresses imposed on the joint are

$$p_c, p_t = \frac{f_a}{2} \pm \sqrt{\frac{f_a^2}{4} + v_j^2} = +4.5, -3.7 \text{ (MPa)} [ +650, -540 \text{ (psi)}] \quad (9)$$

Normalizing these results in terms of the nominal design concrete compressive strength of,  $f'_c$ , 34.5MPa (5ksi), yields the normalized principle compressive,  $p_c$ , and tensile stresses,  $p_t$ , of  $0.13f'_c$  and  $0.63\sqrt{f'_c} \text{ (MPa)} [7.56\sqrt{f'_c} \text{ (psi)}]$ , respectively. With this level of principle compressive stresses significantly lower than  $0.30 f'_c$  the bent cap size was adequate in preventing crushing of the joint diagonal compression strut. Joint principle tensile stresses,  $p_t$ , were computed using the entire moment curvature envelope shown in Figure 4(a). As shown in Figure 4(b), results indicate that the principle tensile stresses,  $p_t$ , significantly exceeded the limits stipulated by Eq. (7) and full joint shear reinforcement was required for design of the joint.

## Joint Reinforcement

Joint design includes the required shear reinforcement in terms of: *i*) top,  $\square A_{tb}$ , and bottom,  $\square A_{bb}$ , additional bent cap longitudinal reinforcement, *ii*) vertical reinforcement outside and inside the joint region,  $A_{jv}$ , and *iii*) horizontal joint reinforcement,  $A_{jh}$ .

## Additional Longitudinal Reinforcement in the Bent Cap

Based on the strut and tie model presented by Sritharan (2005), the area of additional top,  $\square A_{tb}$ , and bottom,  $\square A_{bb}$ , longitudinal reinforcement required was

$$\Delta A_{tb} = 0.175 \lambda_o A_{sc} \frac{f_{y,c}}{f_{y,b}} \quad (10)$$

$$\Delta A_{bb} = 0.15 \lambda_o A_{sc} \frac{f_{y,c}}{f_{y,b}} \quad (11)$$

It is required that this reinforcement be provided in addition to the reinforcement required to increase the bent cap yield capacity. The references to top and bottom longitudinal reinforcement are for a bent cap in its upright position, and in the units these are inverted.

Using a column longitudinal reinforcement of 12-D32 (#10) with a tested grade,  $f_y$ , of 519MPa (75.3MPa), a tested grade for the additional bent cap longitudinal reinforcement (D19-#6) of 493MPa (71.5ksi), along with using  $\square_o = 1.0$ , the required limits for  $\square A_{tb}$  and  $\square A_{bb}$  were 1759mm<sup>2</sup> (2.73in.<sup>2</sup>) or 7-D19 (#6) and 1552mm<sup>2</sup> (2.41in.<sup>2</sup>) or 6-D19 (#6), respectively. From the bent cap longitudinal reinforcement provided, subtracting the reinforcement designed for the flexural capacity of the bent cap, 9-D19 (#6) and 7-D19 (#6) were available for  $\square A_{tb}$  and  $\square A_{bb}$ , respectively, which exceeds the required 7 and 6 bars.

## Additional Joint Shear Reinforcement

The area of interior vertical joint shear reinforcement,  $A_{jv}^{int}$ , was (Sritharan, 2005)

$$A_{jv}^{int} = 0.095 \lambda_0 A_{sc} \frac{f_{y,c}}{f_{y,v}} \quad (\text{Internal}) \quad (12)$$

Where  $f_{y,v}$  is the yield stress of the vertical stirrups. In addition, an area of external vertical joint shear reinforcement was placed at a distance  $H_b$  away from the column face and is

$$A_{jv}^{ext} = 0.125 \lambda_0 A_{sc} \frac{f_{y,c}}{f_{y,v}} \quad (\text{External}) \quad (13)$$

For the design of the internal and external joint shear reinforcement D13 (#4) closed stirrups were used and the tested grade was 506MPa (73.4ksi). As such the required  $A_{jv}^{int}$  was 958mm<sup>2</sup> (1.48in.<sup>2</sup>) or 8 legs of D13 (#4), and  $A_{jv}^{ext}$  was 1261mm<sup>2</sup> (1.95in.<sup>2</sup>) or 10 legs of D13 (#4), respectively. Outside the joint region and within a distance of  $H_b$ , four D13 (#4) closed stirrups were provided on either side of the existing bent cap and within the joint three D13 (#4) stirrups were provided on either side of the existing bent cap, which exceeds the required reinforcement to satisfy  $A_{jv}^{int}$  and  $A_{jv}^{ext}$ , respectively.

### **Transverse Reinforcement Unit 1**

Although not continuous, the transverse headed reinforcement in Unit 1 was extended halfway into the bent cap to form a mechanism to confine the concrete in the joint region due to insufficient detailing of the as-built section. This headed reinforcement was also effective in ensuring composite action between the as-built and the new section. As shown in Figure 2(b) and (e), horizontal D13 (#4) closed stirrups were also placed across the top and outside of the joint region to confine this portion of the new section. To prevent pullout of the column reinforcement, Priestley *et al.* (1995) recommends limiting the strain in the concrete to 0.0015, which also leads to limiting the strain in the reinforcing hoops to 0.0015. Typically this strain value is below the yield strain and force equilibrium results in

$$A_{st} 0.0015E_s = 0.23A_{sc}\lambda_o f_{yc} \quad (14)$$

Using the tested ultimate strength of the column longitudinal reinforcement of 671MPa (97.3ksi) and the tested modulus of elasticity of 188.9GPa (27,398ksi), yields a required transverse reinforcement area,  $A_{st}$ , of 5355 mm<sup>2</sup> (10.23in.<sup>2</sup>). As such, 33-D16 (#5) headed reinforcing bars were provided giving a total of 6600 mm<sup>2</sup> (8.30in.<sup>2</sup>).

Figure 2(e) shows the final retrofit cross-section with the longitudinal reinforcement provided to increase the elastic moment capacity and additional transverse and vertical shear reinforcement. The spacing of the stirrups and headed reinforcement are shown in Figure 2(a).

In addition, vertical headed reinforcement was also installed from the top surface of the bent cap, see Figure 2(b) and (d). According to this detail the vertical headed reinforcement extended to a depth equal to the embedded length of the column longitudinal reinforcement. This reinforcement was placed near the center of the as-built bent cap, see Figure 2(e), to ensure proper transfer of forces from the column longitudinal reinforcement to the vertical headed reinforcement by means of the diagonal struts shown in Figure 5.

### **Modifications in the Reinforcement Layout for Unit 2**

Following testing of Unit 1 a few modifications were implemented for Unit 2. In Unit 1 the horizontal headed reinforcement was installed in two pieces from either side of the bent cap, see Figure 2(b). Although this detail provided for an easier construction, it was not sufficient in preventing excessive dilations in the transverse direction. As such, in Unit 2, the horizontal headed reinforcement was installed as a single continuous piece. At one end a head was welded to the rebar and at the other end threads were used to fasten the closing head. Figure 3(a) shows the continuous headed reinforcement running through the transverse direction of the bent cap.



During testing of Unit 1, onset of buckling of the column longitudinal reinforcement initiated soon after crushing of the cover concrete in the gap region. In order to improve the anti-buckling resistance for the longitudinal reinforcement, two additional D-13 (#4) field welded hoops were also provided within the steel shell gap region, as shown in Figure 3(a) and (b).

Finally, during the final stages of testing of Unit 1 wide open cracks were observed in the bent cap top surface near the column interface. As such, the following modifications were implemented: *i*) an additional headed rebar was installed through the gap region and within the column longitudinal reinforcement, and *ii*) one additional D13 (#4) closed stirrup was provided on either side of the bent cap running through the column and within the steel shell gap region, see Figure 6(b).

### **Modifications in the Reinforcement Layout for Unit 3**

The upgrade scheme was slightly modified for the third unit. Post-tensioned rods instead of the horizontal headed reinforcement were used in the joint region, as shown in Figure 3(c) and Figure 6(c). Transverse prestressing is a feasible alternative for increasing the strength of the joint, because it actively confines the concrete and induces an increase in the bond strength provided to the column longitudinal reinforcement. In addition, the steel shell gap was reduced from 52mm (2in.) to 13mm (0.50in.), to further reduce the propensity for buckling of the column longitudinal reinforcement. The remaining reinforcement layout was identical to Unit 2, and the retrofitted cross-section reinforcing layout for Unit 3 is shown in Figure 3(c) and Figure 6(c).

### **Installation of the Headed Reinforcement**

The headed reinforcement was epoxied to the as-built section by using U.S Anchor Corp.'s HS-200 epoxy a rapid setting high strength structural epoxy. In order to accomplish this, holes were predrilled in the as-built specimen and cleaned with compressed air. Then the epoxy was injected

into each hole until it was approximately half full. The rebar was inserted with a slow twisting motion to avoid any air voids. The installed headed reinforcement for the three units is shown in Figure 6. After the epoxy cured, the retrofit longitudinal and vertical steel was tied in place as shown in Figure 6. The bent cap was then formed and the retrofit concrete was poured.

## **LOADING PROTOCOL**

The test units were first subjected to single cycles under *force control* at 25%, 50%, 75% and 100% of the theoretical first yield. As shown in Figure 7, after reaching first yielding, the units were then loaded under *displacement control* with three cycles applied at each of the predefined displacement ductility levels of 1, 1.5, 2, 3, 4, 6, 8, and 10.

## **EXPERIMENTAL RESULTS – UNIT 1**

Key experimental results for Unit 1 are shown in Figure 8. After testing, the displacement ductility at level one was rectified to reflect directly the test results. Based on a direct investigation of the test results the displacement at ductility 1 was reset to 31.5mm (1.24in.), leading to the ductility levels shown in Figure 8(a).

Figure 9(a) shows the normalized peak load levels as a function of the theoretical yield,  $V_y$ , and at the different displacement cycles for the three test units. In Figure 9(a), it is clear that the maximum lateral load was recorded during loading to the first cycle to displacement 152.4mm (6.0in.) or ductility 5. From the first to the second cycle the drop in the lateral load was approximately 17%, whereas from the second to the third cycle the drop in the lateral load was only 5%. In addition, from the third cycle at 152.4mm (6.0in.) to the first cycle at 228.6mm (9.0in.), the registered levels of strength degradation were less than 5% indicating stabilization in the lateral response of the test unit. This suggests that at this level any damage that has developed

within the joint region stabilized, and the reinforcement provided in the new bent cap section was effective in preventing further degradation to the test unit.

In Figure 8(a), during subsequent loading to the second and third cycle at ductility 7, excessive levels of strength degradation were observed in combination with pinching in the hysteretic response. These two cycles mark the first significant drop in the lateral load below  $V'_y$ . Before this displacement ductility level, the hysteretic response of the test unit was reasonably stable with significant amounts of energy dissipation capacity. Figure 8(b) shows minimum diagonal cracking within the joint region, whereas Figure 8(c) shows significant damage in the top surface of the bent cap and in the vicinity of the column. As previously stated, it is important to emphasize that during loading to the first cycle at ductility 7 the lateral load was nearly the same as the load registered to the third cycle at ductility 5. This indicates that load transfer within the joint region was still within limits capable of sustaining load levels within 80% of the maximum registered lateral load for ductility levels less than 5.

## **EXPERIMENTAL RESULTS – UNIT 2**

Unit 2 was tested following the loading protocol shown in Figure 7 and the load deformation response of Unit 2 is shown in Figure 10(a). As in Unit 1, based on a direct investigation of the test results the new displacement at ductility 1 was also set at 31.5mm (1.24in.). This figure shows that Unit 2 response displayed similar features as those described for Unit 1. By comparing the load deformation response for these two test units, one may conclude that the response of Unit 2 displayed an improvement in the seismic response in terms of damage and load degradation at higher ductility levels.

In Unit 2 the maximum registered lateral load was also recorded during the first cycle to ductility 5, while achieving slightly higher load levels than Unit 1. Figure 9(a) shows that

between the first and second cycles at 152.4mm (6.0in.) the drop in the lateral load was the same as in Unit 1 or 17%, and between the second and third cycles the drop in the lateral load was also 5%, indicating once again stability in the response of this unit. This indicates that up to peak load the performance of units 1 and 2 was nearly the same.

Figure 9(a) clearly shows that compared to Unit 1, Unit 2 experienced lower levels of strength degradation at 228.6mm (9.0in.). This is one of the relevant differences between the performances of these two test units. As before, the unit exhibit significant levels of strain penetration around the column but this was limited to the first row of vertical headed reinforcement. Compared to Unit 1, Unit 2 experienced also lower levels of damage in the bent cap as shown in Figure 10(c). In addition, cracking due to joint shear was minimal and all joint shear cracks were small as shown in Figure 10(b).

Unlike Unit 1, the first significant drop in the lateral load capacity of the test unit below the theoretical yield load level was not observed until the first cycle to ductility 10. However, it is important to recognize that, when loading to ductility 7 and during the pull direction to the third cycle, low cycle fatigue fracture of the longitudinal reinforcement was observed. This is a clear indication that the loss in the strength of the test unit during the last cycles was predominantly due to fracture of the longitudinal reinforcement. In total, four column longitudinal bars fractured due to low cycle fatigue indicating reserve capacity against pullout of the column reinforcement.

### **EXPERIMENTAL RESULTS – UNIT 3**

The load deformation response of Unit 3 is shown in Figure 11(a). For Unit 3 and based on a direct investigation of the test results the displacement at ductility 1 was set at 42.1mm (1.66in.), translating in the displacement ductility levels shown in the Figure 11(a).

Test results clearly indicate that reducing the steel shell gap to 13mm (1/2in.) prevented excessive crushing of the concrete cover, and buckling of the column longitudinal bars, as observed in Unit 1 and 2. Cracking on the sides of the bent cap resulting from joint shear was minimal and all cracks stayed small as shown in Figure 11(b), and damage above the bent cap was nearly the same as in Unit 2, see Figure 11(c). However, the crack pattern was more distributed than in Units 1 and 2.

In Unit 3 the maximum registered lateral load was also recorded during the first cycle to ductility 4. Results presented in Figure 9(a) show that Unit 3 peak loads were nearly 20% higher than those registered for the previous two units. This figure also shows that between the first and second cycles at 152.4mm (6.0in.) the drop in the lateral load was approximately 14%, and between the second and third cycles the drop in the lateral load was 5%, indicating once again stability in the response of Unit 3.

The first significant drop in the lateral load capacity of Unit 3 below the theoretical first yield load level was observed during the third cycle to ductility 6, see Figure 11(a). This indicates similar levels of load degradation, indicating that reducing the steel shell gap did not translate directly into an improvement of the seismic response of the test unit. This suggests that the steel shell gap should not be reduced below levels that can lead to significant increase in the load capacity of the unit, leading to higher principle tensile stress demands in the joint.

## **DISCUSSION OF THE EXPERIMENTAL RESULTS**

Comparison in the response of the three test units was described in Figure 9(a) and further discussions of the test results is presented in terms of the hysteretic energy dissipation capacity for the three test units. The energy dissipated through the structural system was calculated from the area of the hysteretic loops at each displacement level and results of these analyses are shown in Figure

9(b). The total cumulative hysteretic energy dissipated for Units 1, 2, and 3 was 986kN-m (727 kips-ft), 1,154kN-m (851kips=ft), and 1,107kN-m (816kips-ft), respectively. These values show that Unit 2 had a slightly higher capacity to dissipate the hysteretic energy by nearly 15% in comparison to Unit 1 and 5% higher in comparison to Unit 3. The higher energy dissipation capacity associated with Unit 2 is evident by the reduced pinching of the hysteresis loops for this unit in comparison to those of Units 1 and 3. This suggests an improved performance for the joint of Units 2 and 3 and hence a greater capacity to dissipate energy. As shown in this figure, Units 2 and 3 consistently dissipated higher levels of energy beyond 228.6mm (9.0in.). Beyond this level the three units displayed similar levels of decrease in dissipated energy.

Although Unit 3 was able to dissipate similar levels of energy as Unit 2, the principle tensile stresses for this unit exceeded those of Unit 2. As such, reducing the steel shell gap from 51mm (2in.) to 13mm (0.50in.) for Unit 3 provided better confinement of the concrete cover; thus, preventing buckling and low cyclic fatigue fracture of the column longitudinal bars. However, the significant increase in the load capacity of Unit 3 led to a matched increase demand in the joint region.

## **CONCLUSIONS**

Overall, experimental results showed that the three test units displayed ductile responses up to ductility 5 without significant decreases in the strength, inelastic actions due to flexural yielding of the bent cap, shear failure of the bent cap or joint shear failure. Priestley *et. al* (1995) recommends that the displacement ductility capacity of multiple column bridge bents should not be less than 4 when composed of columns with an aspect ratio of 4.5. Experimental results clearly indicate that the displacement ductility levels achieved are within the recommended values.

Beyond the ductility level of 5, the main failure mode of Unit 1 was attributed to joint shear failure due to excessive transverse dilations within the joint region. This was attributed to the discontinuity of the transverse horizontal headed reinforcement through the joint region. As such, it is recommended not to use this detail in regions prone to seismic events.

An improved joint detail was implemented for Units 2 and 3, in which the transverse reinforcement was made continuous through the joint region. In Unit 2, the main failure mode was attributed to low cyclic fatigue of the column longitudinal reinforcement, with extensive joint degradation recorded beyond ductility 7. In Unit 3 the joint was post-tensioned in the transverse direction while also decreasing the gap length between the steel shell and the bent cap. Beyond ductility 7 degradation of the lateral load capacity of the column occurred due to joint shear failure. This observation suggests that in design practice combining details of Units 2 and 3 are likely to lead to an improved joint performance. As such in future research, it is advisable to investigate an increase in the gap region to 38.1mm (1.5in.).

Based on the experimental results the research team proposes that a ductility of 4 be implemented in design using the details proposed for Units 2 and 3. At this level some strength degradation is expected, but will neither cause significant decrease in the column axial capacity nor cause significant wide open cracks in the joint region. In addition, for columns with lower reinforcement ratios or deeper bent cap the full dependable moment capacity and displacement ductility of the column can be expected to develop. As such, for these columns higher displacement ductility levels may be accepted for assessment investigation.

## **ACKNOWLEDGEMENTS**

The research project described in this paper was funded by the Alaska Department of Transportation and Public Facilities, and the University Transportation Center located at UMR.

## NOTATIONS

$A_{ci}$	= individual segment area for the concrete infill
$A_{jv}^{ext}$	=area of external vertical joint shear reinforcement
$A_{jv}^{int}$	=area of internal vertical joint shear reinforcement
$A_{sc}$	= total area of the column longitudinal reinforcement
$A_{si}$	= individual area for a single reinforcing bar
$A_{shi}$	=individual segment area for the steel shell
$A_{st}$	=total transverse reinforcement area
$D_c$	=outside diameter of the CISS foundation shaft
$D_c'$	= diameter of the column concrete core
$E_s$	= reinforcing steel modulus of elasticity
$H_b$	=depth of the bent cap
$M_y'$	=first yield moment capacity
$M_u$	=ultimate moment capacity
$P$	=applied axial load
$W_b$	=width of the bent cap
$d_b$	=diameter of the column longitudinal reinforcement
$l_d$	=development length of the longitudinal reinforcement
$f_a$	=joint axial stress
$f_{ci}$	=internal stresses for the concrete infill
$f_c'$	=concrete compression strength
$f_{c,b}'$	=concrete compression strength for the bent cap
$f_{shi}$	=internal stresses for the steel shell
$f_{si}$	=internal stresses for the reinforcing bars
$f_{y,b}$	=yield strength of the bent cap longitudinal reinforcement
$f_{y,c}$	=yield strength of the column longitudinal reinforcement
$f_{y,v}$	=yield strength of the joint shear reinforcement
$nc$	= number of concrete segments
$ns$	= number of reinforcing bars



- $p_c$  =principle compressive stress
- $p_t$  =principle tensile stress
- $v_j$  =joint shearing stress
- $A_{tb}$  = area of additional bottom longitudinal reinforcement
- $A_{tb}$  = area of additional top longitudinal reinforcement
- $\alpha_i$  =stress factor, equal to one if in compression, or zero if in tension
- $\phi_o$  =over-strength factor; 1.4 when design yield stress is used, otherwise  $\phi_o = 1.0$
- $\rho$  = reinforcement ratio

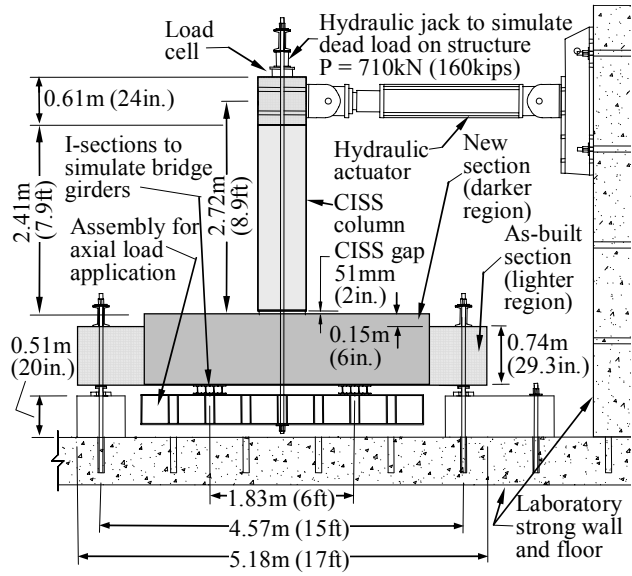
## REFERENCES

- Alcocer, S., and Jirsa, J. O. (1993), "Strength of Reinforced Concrete Frame Connections Rehabilitated by Jacketing," *ACI Structure Journal*, Vol. 90, No. 3, pp.249-261
- American Association of State Highway and Transportation Officials (AASHTO) (1998), "AASHTO LRFD Bridge Design Specifications," 2nd Edition, Published by the Association, Washington, DC, 1102 pp.
- American Concrete Institute (ACI), (2005), "Building Code Requirements for Structural Concrete," ACI318-2005, Farmington Hills, MI.
- California Department of Transportation (Caltrans), (2004), "Caltrans Seismic Design Criteria," Caltrans SDC Version 1.3, Sacramento, CA, February 2004.
- Ingham, J. M., Priestley, M. J .N., and Seible, F. (1994). "Seismic Performance of Bridge Knee Joints – Volume I," *Rep. No. SSRP 94/12*, University of California San Diego.
- Pantelides, C.P., Alameddine, F., Sardo, T., and Imbsen, R.A. (2004), "Street Bridge on Interstate 80," *ASCE Journal of Bridge Engineering*, Vol. 9, no. 3, July-August 2004, pp. 333-342.

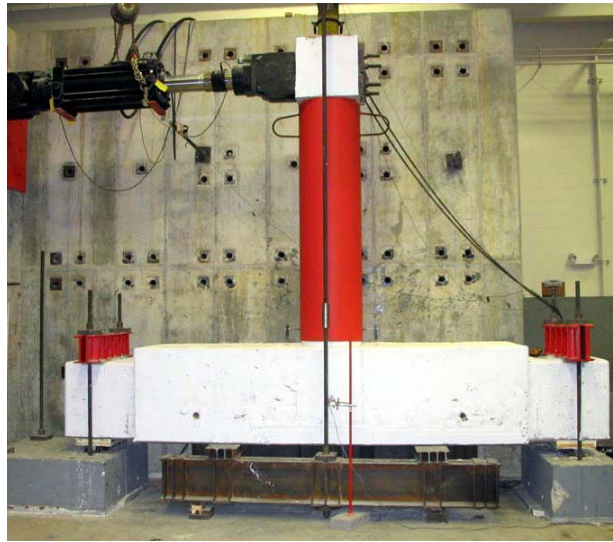
- Priestley, M. J. N.; Seible, F.; and Anderson, D. L. (1993), "Proof Test of a Retrofit Concept for the San Francisco Double-Deck Viaducts: Part 1— Design Concept, Details, and Model," *ACI Structural Journal*, V. 90, No. 5, pp. 467-479.
- Priestley, M. J. N., Seible, F., and Calvi, M. (1995), *Seismic Design and Retrofit of Bridges*, John Wiley & Sons, Inc., New York, NY, Sep 1995, 672 pp.
- Silva, Pedro F., Sritharan, S., Seible, F., Priestley, M.J.N. (1999), "Full-Scale Test of the Alaska Cast-In-Place Steel Shell Three Column Bridge Bent", Division of Structural Engineering, University of San Diego, La Jolla, California, February 1999, Report # SSRP-98/13
- Silva, P.F., and Seible, F. (2001), "Seismic Performance Evaluation of CISS Piles," *ACI Structural Journal*, Vol. 98, No. 1, pp. 36-49.
- Silva, P.F., Ereckson, N.J., and Chen, G. (2007), "Seismic Retrofit of Bridge Joints in the Central U.S. with CFRP Composites," *ACI Structural Journal*, Vol. 104, No. 2, pp. 207-217
- Sritharan, S. (2005), "Improved Seismic Design Procedure for Concrete Bridge Joints," *ASCE Journal of Structural Engineering*, Vol. 131, No. 9, pp. 1334–1344.

## **LIST OF FIGURES**

- Figure 1. Test Setup
- Figure 2. As-Built and Unit 1 Reinforcement Layout
- Figure 3. Units 2 and 3 Reinforcement Layout
- Figure 4. Member Analysis
- Figure 5. Formation of Outside Diagonal Strut
- Figure 6. New Bent Cap Section Reinforcement Layout (Side View)
- Figure 7. Loading Sequence
- Figure 8. Unit 1 – Key Experimental Results
- Figure 9. Comparison in Response for the Three Test Units
- Figure 10. Unit 2 – Key Experimental Results
- Figure 11. Unit 3 – Key Experimental Results

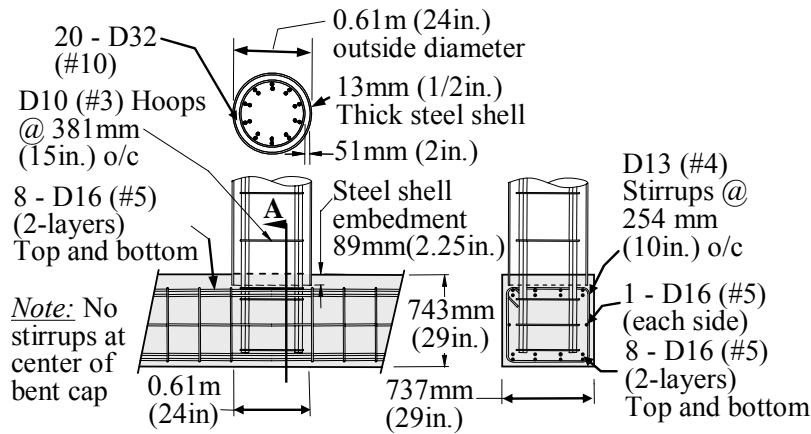


(a) Test Setup Schematics

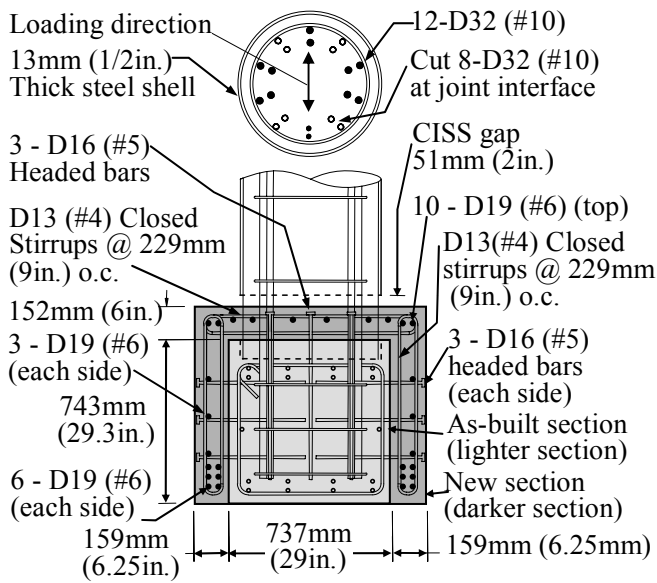


(b) Unit 1 Ready for Testing

**Figure 1. Test Setup**



(a) As-Built Reinforcement Layout



(b) Unit 1 Reinforcement Layout



(c) Unit 1

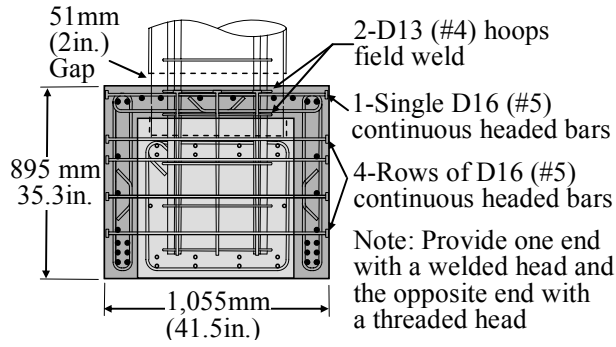


(d) Installation of Headed Bars



(e) New Reinforcement

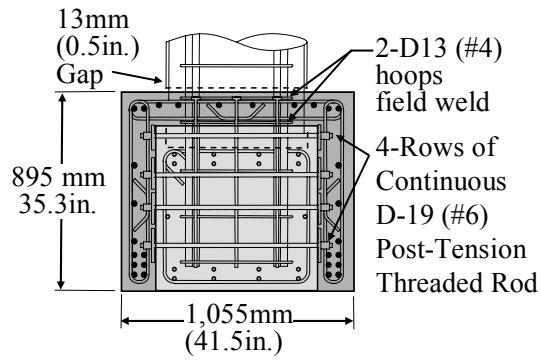
Figure 2. As-Built and Unit 1 Reinforcement Layout



(a) Unit 2 Reinforcement Layout



(b) Unit 2 CISS above Bent Cap Interface

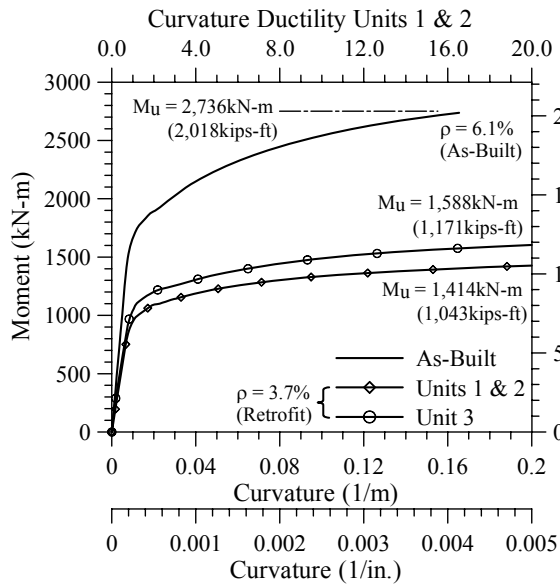


(c) Unit 3 Reinforcement Layout

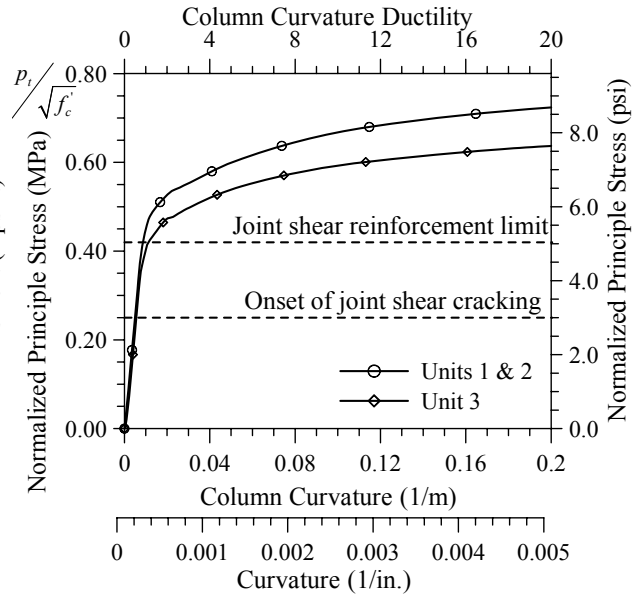


(d) Unit 3 CISS above Bent Cap Interface

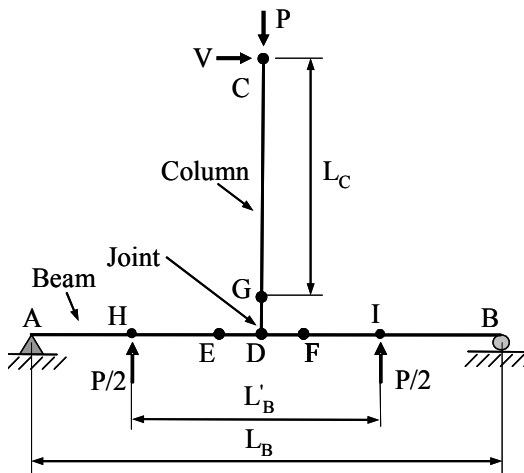
**Figure 3. Units 2 and 3 Reinforcement Layout**



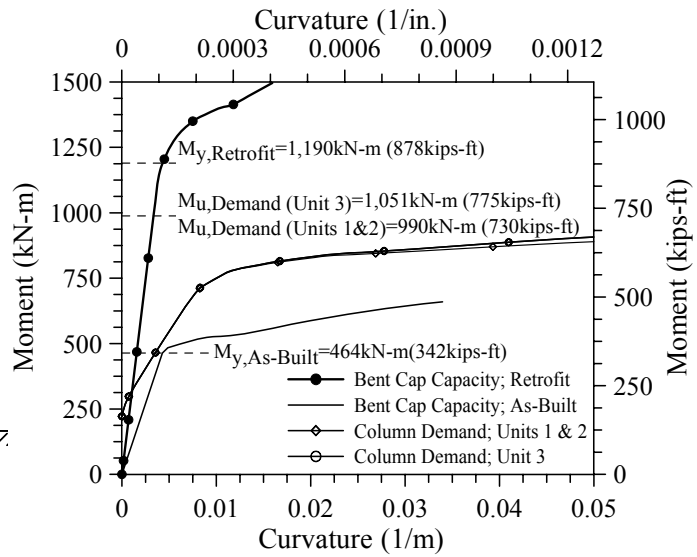
(a) Column Analysis



(b) Joint Analysis



(c) Analytical model



(d) Bent Cap Analysis

Figure 4. Member Analysis

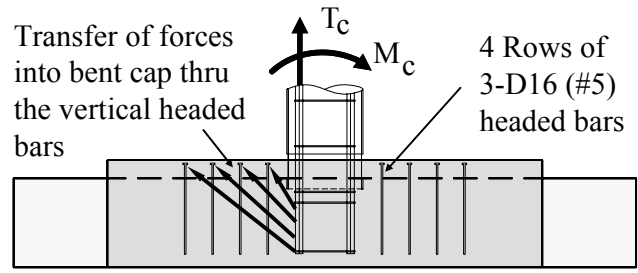


**Figure 5. Formation of Outside Diagonal Strut**



**(a) Unit 1**

**(b) Unit 2**

**(c) Unit 3**

**Figure 6. New Bent Cap Section Reinforcement Layout (Side View)**



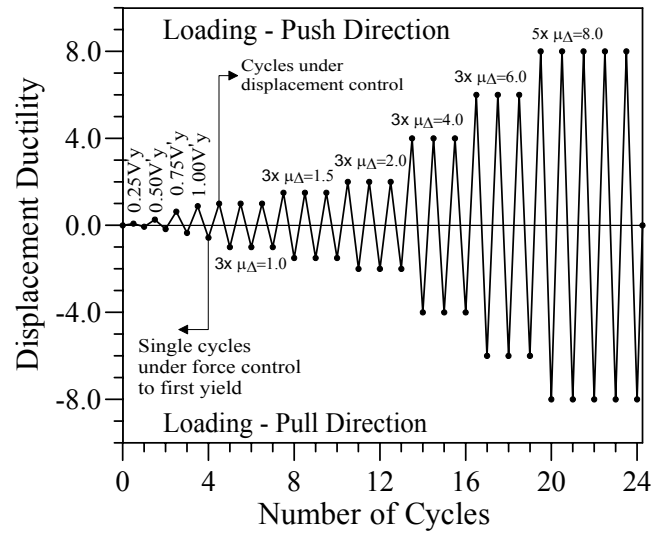
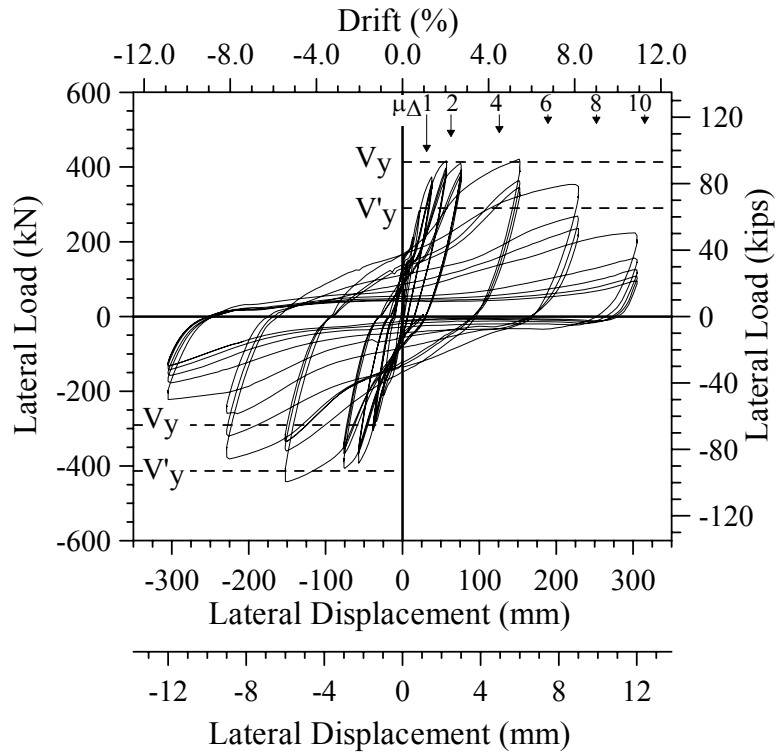
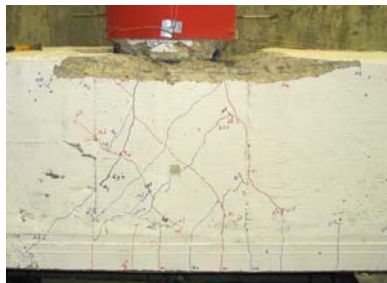


**Figure 7. Loading Sequence**



(a) Load-Deformation Response

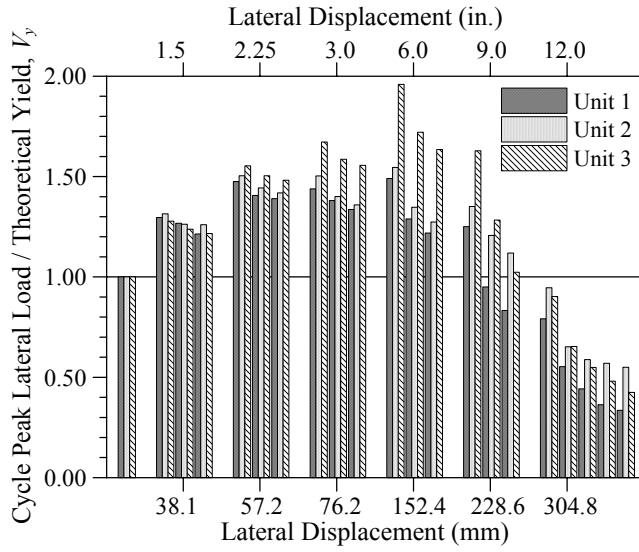


(b) Joint Damage

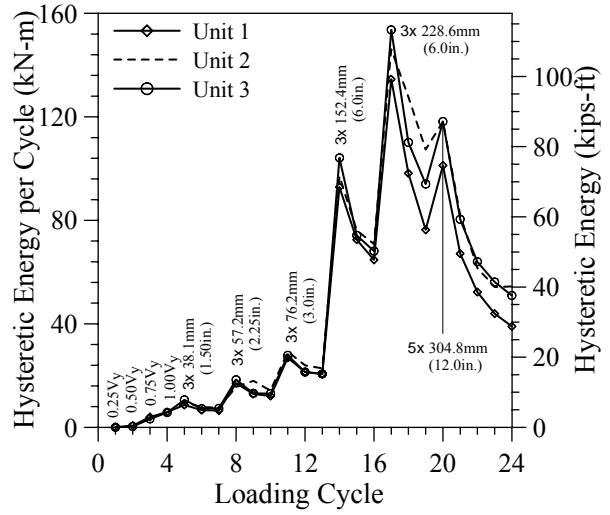


(c) Bent Cap Damage

**Figure 8. Unit 1 – Key Experimental Results**

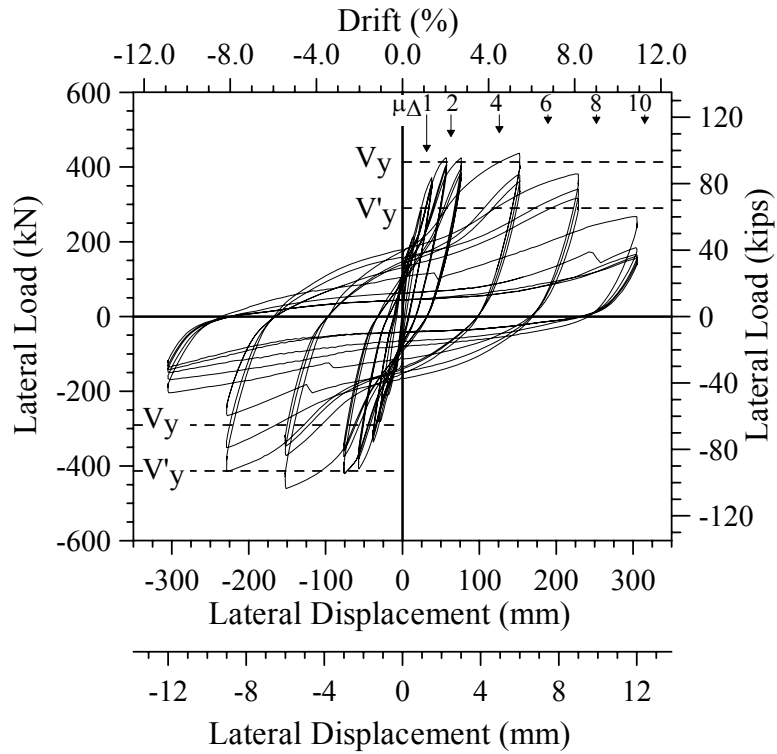


(a) Strength Degradation



(b) Cumulative Dissipated Energy

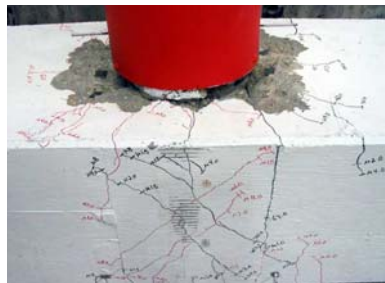
**Figure 9. Comparison in Response for the Three Test Units**



(a) Load-Deformation Response

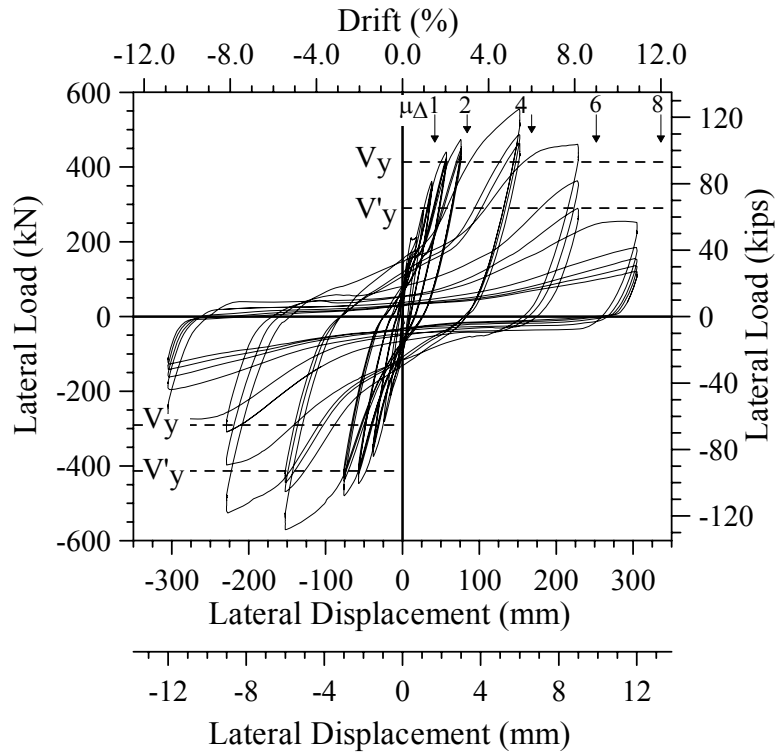


(b) Joint Damage

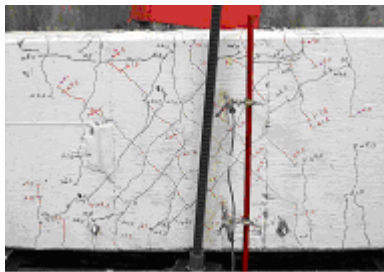


(c) Bent Cap Damage

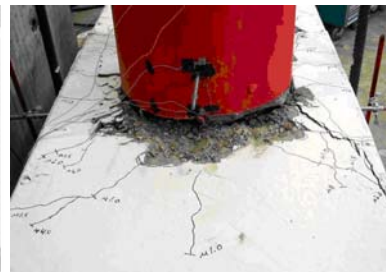
**Figure 10. Unit 2 – Key Experimental Results**



(a) Load-Deformation Response



(b) Joint Damage



(c) Bent Cap Damage

**Figure 11. Unit 3 – Key Experimental Results**

**Table 1. Concrete Material Properties**

Unit No.	Test *	Column		As-Built Bent Cap		Retrofit Bent Cap	
		MPa	(ksi)	MPa	(ksi)	MPa	(ksi)
1	28 Day	27.1	3.9	29.0	4.2	33.8	4.9
	Day of Test	29.3	4.2	33.8	4.9	36.9	5.4
2	28 Day	28.0	4.1	33.5	4.9	36.6	5.3
	Day of Test	30.8	4.5	38.3	5.6	38.9	5.6
3	28 Day	39.3	5.7	26.2	3.8	36.6	5.3
	Day of Test	43.7	6.3	27.1	3.9	38.8	5.6

\* Specified nominal strength was 34.5MPa (5ksi)

**Table 2. Reinforcing Steel Material Properties – As-built Section**

Unit No.	Bar Size	Bar Location	$f_y$		$f_u$	
			MPa	(ksi)	MPa	(ksi)
1 and 2	D10 (#3)	Column Hoops	310	45.0	474	68.7
	D13 (#4)	Bent Shear	425	61.6	638	92.5
	D16 (#5)	Bent Longitudinal	554	80.4	689	99.9
	D32 (#10)	Column Longitudinal*	519	75.3	671	97.3
3	D10 (#3)	Column Hoops	435	63.1	632	91.7
	D13 (#3)	Bent Shear	503	73.0	669	97.0
	D16 (#3)	Bent Longitudinal	476	69.0	702	101.8
	D32 (#3)	Column Longitudinal	497	72.1	746	108.2

\* Calculated yield strain of 2,740  $\mu\epsilon$

**Table 3. Reinforcing Steel Material Properties – Retrofit Section**

Unit No.	Bar Size	Bar Location	$f_y$		$f_u$	
			MPa	(ksi)	MPa	(ksi)
1	D13 (#4)	Bent Shear	506	73.4	674	97.8
	D16 (#5)	Bent Transverse	486	70.5	652	94.6
	D19 (#6)	Bent Longitudinal	493	71.5	775	112.4
2	D13 (#4)	Bent Shear	503	73.0	669	97.0
	D16 (#5)	Bent Transverse	476	69.0	645	93.5
	D19 (#6)	Bent Longitudinal	472	68.5	696	100.9
3	D13 (#4)	Bent Shear	506	73.4	674	97.8
	D16 (#5)	Bent Transverse	486	70.5	652	94.6
	D19 (#6)	Bent Longitudinal	493	71.5	775	112.4
	D19 (#6)*	Pre-Stress Rods	517	75.0	689	99.9

\* Threaded Rod, Manufacturer's Specifications

**Table 4. Bent Cap Flexural Design Considerations**

Item	Units 1 & 2 kN-m (kips-ft)	Unit 3 kN-m (kips-ft)
$M_u$ Column Capacity	1,414 (1043)	1,588 (1,171)
$M_u$ Column Transformed	990 (730)	1,051 (775)
$M_y$ As-Built Bent Cap	464 (342)	
$M_y$ New Section Bent Cap	1,190 (878)	